Correlation of Turbulent Trailing Vortex Decay Data

James D. Iversen*
Iowa State University, Ames, Iowa

A correlation function, derived on the basis of self-similar variable eddy-viscosity decay, is introduced and utilized to correlate aircraft trailing vortex velocity data from ground and flight experiments. The correlation function collapses maximum tangential velocity data from scale-model and flight tests to a single curve. The resulting curve clearly shows both the inviscid plateau and the downstream decay regions. A comparison between experimental data and numerical solution shows closer agreement with the variable eddy viscosity solution than the constant viscosity analytical solution.

Nomenclature

a = Squire's coefficient [Eq. (1)]
$Æ$ = aspect ratio, b^2/S
b = wing span
ℓ = mixing length
N = similarity variable, $r^2/4\gamma_0 t$
r = vortex radial coordinate
r_1 = vortex core radius (at maximum tangential speed)
r_0 = initial core radius
S = wing area
t = time
U_∞ = freestream speed
V = tangential vortex speed
V_1 = maximum tangential vortex speed
x = distance downstream from generating aircraft
α = mixing length proportionality constant
γ = reduced circulation, rV
γ_0 = γ at large radius
Γ = circulation, $2\pi\gamma$
Γ_1 = circulation at core radius
Γ_0 = circulation at large radius
Λ^2 = proportionality constant [Eq. (2)]
v = kinematic viscosity
v_T = turbulent eddy viscosity

Introduction

A CORRELATION function is introduced and utilized to correlate aircraft trailing vortex velocity data from ground and flight experiments. Recent water channel tests by Ciffone and Orloff[1] have identified two distinct streamwise regions in the decay of trailing vortices. The near-field is an essentially inviscid "plateau" region, existing for some distance downstream, after rollup, in which vortex decay is very slow. Farther downstream, the vortex decays as a function of the square root of downstream distance, as would be expected from a similarity-type solution.

Since the water-channel data and existing wind-tunnel test results concerning trailing vortices have been obtained at relatively low Reynolds numbers, a search was initiated for a correlation function that would substantiate ground-based scale-model data by comparison with large Reynolds number flight tests. The correlation function introduced here is derived on the basis of self-similar turbulent decay of a line vortex. Since the function is based on similarity of an isolated, infinitely long vortex, it would be expected to hold strictly

*Professor, Department of Aerospace Engineering, Engineering Research Institute. Member AIAA.

only for the similarity region far downstream of the generating aircraft, where three-dimensional effects would be negligible, and provided the vortex core radius is significantly smaller than the distance between the vortices. However, it is shown that the similarity parameter can be manipulated (considering plateau-region vortex characteristic) so that maximum tangential velocity data from a large range of Reynolds numbers can be collapsed to one curve. The final result clearly illustrates both the near-field plateau region and the downstream decay region.

The correlation function is derived by numerical solution of the similarity differential equation, using a variable eddy viscosity model. The only empiricism involved is the evaluation of a mixing-length proportionality factor by using large Reynolds number flight data in the similarity region. The correlation function substantiates the validity of small Reynolds number experiments as long as they are correctly interpreted and should aid in understanding the turbulent vortex decay problem.

Eddy Viscosity and Circulation Relationship

Squire[2] hypothesized that, since the principal permanent characteristic of the line vortex is the circulation for large radius Γ_0, the eddy viscosity v_T could be assumed to be proportional to Γ_0, i.e.,

$$v_T = a\Gamma_0/2\pi = a\gamma_0 \qquad (1)$$

Since Eq. (1) is equivalent to the assumption of a constant-eddy viscosity that is independent of radius, the solution[3] for laminar viscous flow could be used, hopefully, to interpret experimental data; it has been so used by various investigators. Owen,[4] partially on the basis of experimental data from various sources, derived an expression for Squire's coefficient a as a surprisingly strong function of Reynolds number (Γ_0/v)

$$a = 2\pi\Lambda^2(\Gamma_0/v)^{1/2} \qquad (2)$$

where Λ^2 was presented as approximately constant.

Decay of Line Vortex

If it is assumed that the flow in a trailing vortex is approximately analogous to the time-dependent flow of an infinite line vortex, then, for variable viscosity, the equation for circulation $\gamma(=rv)$ can be written

$$\partial\gamma/\partial t = r(\partial/\partial r)[v_T r(\partial/\partial r)(\gamma/r^2)]$$
$$+ 2v_T r(\partial/\partial r)(\gamma/r^2) \qquad (3)$$

Assume that the flow is similar, so that $\gamma = \gamma(N)$, where $N = r^2/4\gamma_0 t$.

Condition 1: If $v_T = v_0$, a constant, the Lamb vortex results

$$\gamma = \gamma_0 (1 - e^{-\gamma_0 N / v_0}) = \gamma_0 (1 - e^{-N/a}) \tag{4}$$

Condition 2: If $v_T = \ell^2 | r \partial / \partial r (\gamma / r^2 | + v$, where ℓ is a mixing length, and v is molecular kinematic viscosity, and eddy viscosity variation more representative of turbulent flows is obtained. For similarity, it is necessary that the mixing length be proportional to radius, $\ell = \alpha r$, which is satisfying on physical grounds and is representative of recent numerical calculation.[5] Equation (3) then becomes

$$-\tilde{\gamma}_{\tilde{N}} = (4 | \tilde{N} \tilde{\gamma}_{\tilde{N}} - \tilde{\gamma} | + v / \alpha^2 \gamma_0) \tilde{\gamma}_{\tilde{N}\tilde{N}} \tag{5}$$

Thus

$$\tilde{\gamma} = \tilde{\gamma} (\tilde{N}, v / \alpha^2 \gamma_0) \quad (N = \alpha^2 \tilde{N}, \gamma = \gamma_0 \tilde{\gamma})$$

where α is either a constant or perhaps a function[5] of v / Γ_0, so that

$$\tilde{\gamma} = \tilde{\gamma}, v / \gamma_0) \tag{6}$$

Solution for Variable Eddy Viscosity

Numerical solutions of Eq. (6), satisfying boundary conditions $\tilde{\gamma}(0) = 0$ and $\tilde{\gamma}(\infty) = 1$, were obtained for values of $\alpha^2 \gamma_0 / v$ ranging from 0.01 to 10000. The solutions approach purely viscous flow for very small values of this parameter, and become independent of molecular viscosity for large values. Equation (6) can be rewritten

$$Vb / \gamma_0 = (b / r) \tilde{\gamma} (N, v / \gamma_0) \tag{7}$$

At the core radius (point of maximum tangential velocity)

$$V_1 b / \gamma_0 = (b / r_1) \tilde{\gamma} (r_1^2 / 4 \gamma_0 t, v / \gamma_0) \tag{8}$$

But $r_1^2 / 4 \gamma_0 t = r_1^2 U_\infty / 4 \gamma_0 x = N_1$, a constant. Thus

$$b / r_1 = (b^2 U_\infty / 4 N_1 \gamma_0 x)^{1/2}$$

and

$$V_1 b / \gamma_0 = [(b / x)(U_\infty b / \gamma_0) / 4 N_1]^{1/2} \tilde{\gamma} (N_1, v / \gamma_0)$$

or

$$(V_1 b / \Gamma_0) [(x / b)(\Gamma_0 / U_\infty b)]^{1/2} = C_0 g (\Gamma_0 / v) \tag{9}$$

Values of the quantity of the left-hand side of Eq. (9) were found from flight data from Refs. 6-9. The average value of 46 data points (far downstream values to ensure that the data points were all in the similarity region) was found to be 5.80, so that C_0 is 5.80 if g is set equal to one for large Γ_0 / v. The maximum value of $(\tilde{\gamma} / \tilde{N}^{1/2})$, corresponding to maximum tangential velocity, was found from the numerical solutions to approach a constant value for large Γ_0 / v of 0.539. Since

$$(Vb / \Gamma_0) [(x / b)(\Gamma_0 / U_\infty b)]^{1/2} = (\tilde{\gamma} / \tilde{N}^{1/2}) / [2(2\pi)^{1/2} \alpha]$$

α is found from the flight data to be 0.01854.

Once α is known, and if it is assumed to be independent of Reynolds number, velocity profiles corresponding to solutions of Eq. (6) can be found for any Reynolds number Γ_0/v. The velocity profile for large Reynolds number is shown in Fig. 1, along with the constant eddy viscosity solution for the same value of maximum tangential speed $(v_T = 0.0000766$ $\Gamma_0)$. Comparisons of the computed variable eddy viscosity profile with experimental data from Refs. 1,6, and 10 are shown in Figs. 2-4, with better agreement than for constant viscosity. Figures 2 and 3 illustrate that the value of the ratio of core-radius circulation to large-radius circulation Γ_1 / Γ_0 is
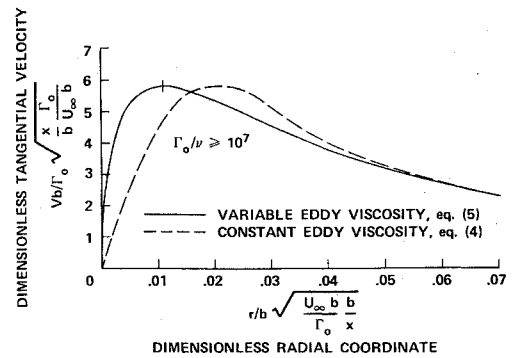

Fig. 1 Vortex velocity profiles, similar solutions, variable and constant eddy viscosity.
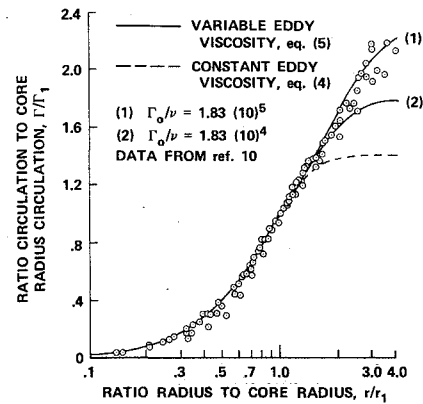

Fig. 2 Circulation profiles, variable and constant eddy viscosity, comparison with experiment.
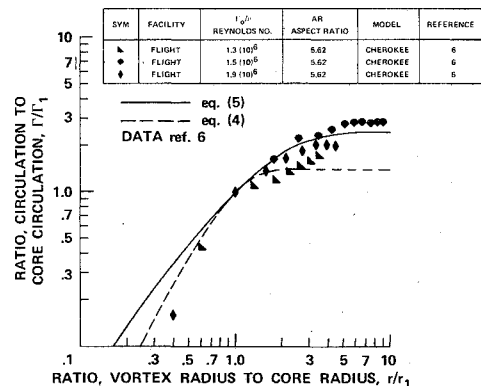

Fig. 3 Circulation profiles, variable and constant eddy viscosity, comparison with experiment.

much larger for the constant eddy viscosity solution than for either the experimental data or the numerical solution of Eq. (5). The large data scatter in Fig. 4 has two causes: 1) Since the data points are instantaneous readings and not time-averaged, turbulence is a factor. 2) If the measuring instrument (in this case a laser-droppler velocimeter) misses the vortex core, then the velocity data will be lower than the desired value on the average and, as shown, most of the scatter falls below the theoretical curve. For this relatively low Reynolds number, a comparison of the velocity profiles for constant and variable eddy viscosities shows that these curves are not far apart; however, the variable viscosity curve seems to represent the data more closely, if the two causes for scatter are taken into account.

Figure 5 shows the variation of circulation with radius for three Reynolds numbers. The left-hand curve is essentially identical to Lamb's solution. The right-hand curve holds for
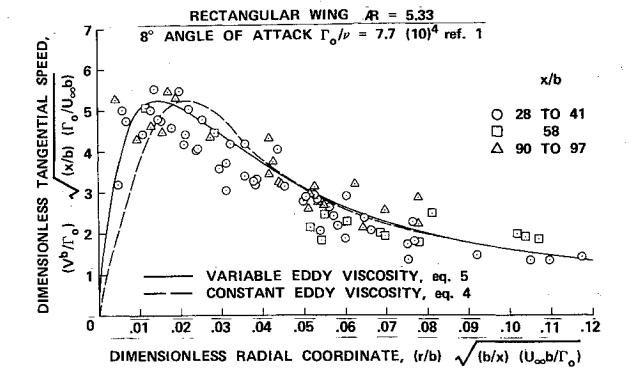
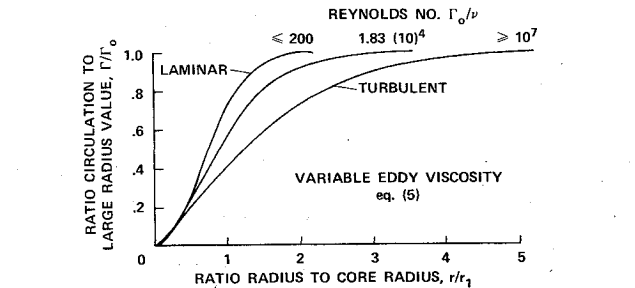**Fig. 4** Vortex velocity profiles, variable and constant eddy viscosity, comparison with experiment.

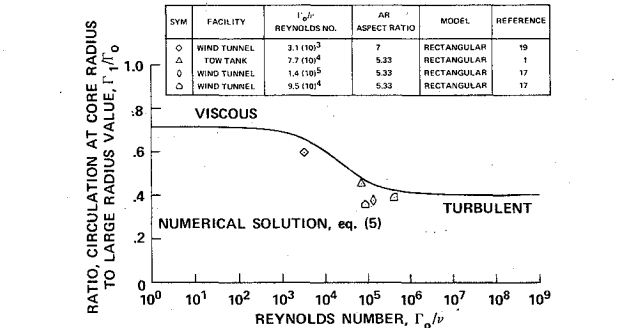**Fig. 5** Circulation profile as function of Reynolds number.

Fig. 6 Core radius circulation vs Reynolds number.

Fig. 7 Core radius velocity vs Reynolds number.

Fig. 8 Core radius vs Reynolds number.

large Reynolds number, and the central curve illustrates an imtermediate Reynolds number example in the region in which eddy and molecular viscosities are of the same order of magnitude. Figure 6 shows the value of circulation at a position of maximum tangential velocity as a function of Reynolds number. Figures 7 and 8 show, respectively, the values of maximum velocity and core radius as a function of Reynolds number. The data points shown in Figs. 6 and 7 substantiate the trends of the numerical solution.

Let us consider the lack of circulation overshoot (i.e., $\bar{\gamma} > 1$) somewhere within the vortex profile (Fig. 5), as predicted by Govindaraju and Saffman[11] and Saffman,[12] for large Reynolds numbers. Govindaraju and Saffman state that the turbulent shear stress tends to zero for large radius faster than $1/r^2$; they obtain an expression for their angular momentum function $J(x)$ dependent upon Reynolds number. According to Saffman's result, the core radius r_1 is proportional to $(v\Gamma_1)^{1/2}t^{1/2}$ for a self-similar vortex, so that $J(x)$ approaches zero for large Reynolds number; this indicates the necessity for circulation overshoot to conserve angular momentum. In the current model, however, the shear stress tends to zero exactly as $1/r^2$ for large radius; thus Saffman's function $J(x)$ remains finite for large Reynolds number. Also, the core radius r_1, for large Reynolds number, is proportional to
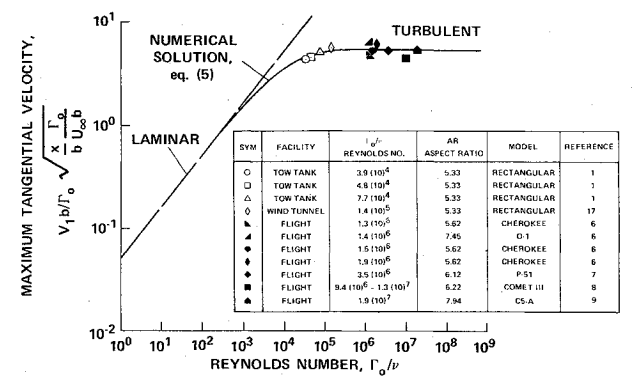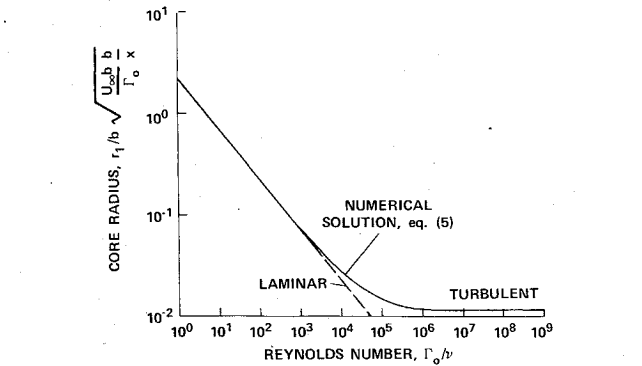
$\Gamma_1^{1/2}t^{1/2}$, which is independent of Reynolds number. The function $J(x)$ then remains finite, as mentioned, and circulation overshoot is not necessary, which agrees with experimental data, as Saffman[12] notes.

Data Correlation

Recent water channel data[1] show that a "plateau" region exists in the vortex trail for some distance aft of the generating aircraft, in which vortex decay is much slower than required for similarity. The characteristics of the plateau region may be at least partly due to nonequilibrium turbulence, and similarity would not be expected to hold until equilibrium is reached. Calculations[5,13] which include nonequilibrium turbulence models show evidence of the plateau region. Velocity profiles of the vortices within the plateau region have been used by Rossow[14] to obtain span loadings by means of an inviscid inverse-Betz method. These span loadings agree well with experimental and theoretical span loadings, which indicates that the plateau-region velocity profiles have not been greatly affected by viscosity or turbulence, except in the relatively small core region.

If similarity is reached far downstream, Eq. (9) should be useful as an experimental correlation parameter. Spreiter and Sacks[15] equated the kinetic energy of rotation per unit length in the plane normal to the flight direction to the induced drag of the wing, and thus found an expression for core radius proportional to wing span. However, the experimental data considered in this investigation do not justify their result. If, instead, it is assumed that the axial momentum deficit in the core is related to the momentum deficit caused by the wing boundary layer, then the core radius must be related to the wing chord, since momentum loss within the wing boundary layer increases with chordwise distance. The best correlation of experimental data in the plateau region (for aspect ratios of 5.33-12) is obtained if it is assumed that the core radius in the plateau region is proportional to the average chord S/b. Then, since the velocity in the vortex would be proportional to centerline circulation Γ_0, for all wings of similar lift

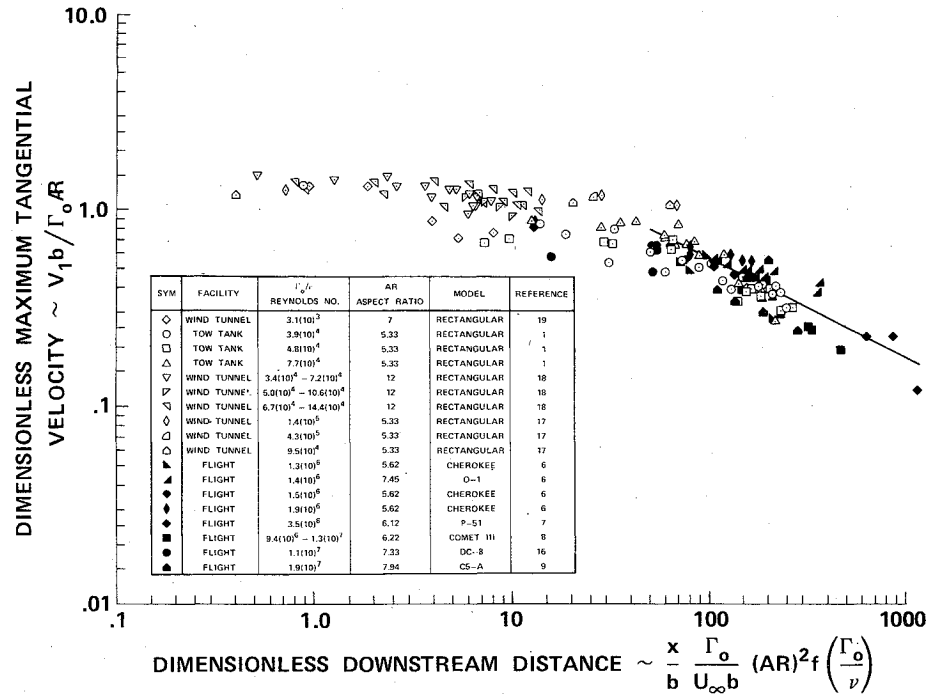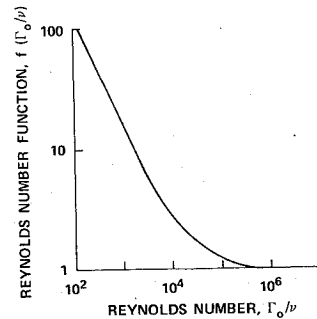**Fig. 9 Correlation curve, core radius velocity vs downstream distance.**

SYM	FACILITY	Γ_0/ν REYNOLDS NO.	AR ASPECT RATIO	MODEL	REFERENCE
◇	WIND TUNNEL	$3.1(10)^3$	7	RECTANGULAR	19
○	TOW TANK	$3.9(10)^4$	5.33	RECTANGULAR	1
□	TOW TANK	$4.8(10)^4$	5.33	RECTANGULAR	1
△	TOW TANK	$7.7(10)^4$	5.33	RECTANGULAR	1
▽	WIND TUNNEL	$3.4(10)^4 - 7.2(10)^4$	12	RECTANGULAR	18
▷	WIND TUNNEL	$5.0(10)^4 - 10.6(10)^4$	12	RECTANGULAR	18
◁	WIND TUNNEL	$6.7(10)^4 - 14.6(10)^4$	12	RECTANGULAR	18
◇	WIND TUNNEL	$1.4(10)^5$	5.33	RECTANGULAR	17
◁	WIND TUNNEL	$4.3(10)^5$	5.33	RECTANGULAR	17
△	WIND TUNNEL	$9.5(10)^4$	5.33	RECTANGULAR	17
◣	FLIGHT	$1.3(10)^6$	5.62	CHEROKEE	6
◢	FLIGHT	$1.4(10)^6$	7.45	O-1	6
●	FLIGHT	$1.5(10)^6$	5.62	CHEROKEE	6
◆	FLIGHT	$1.9(10)^6$	5.62	CHEROKEE	6
◆	FLIGHT	$3.5(10)^6$	6.12	P-51	7
■	FLIGHT	$9.4(10)^6 - 1.3(10)^7$	6.22	COMET III	8
●	FLIGHT	$1.1(10)^7$	7.33	DC-8	16
▲	FLIGHT	$1.9(10)^7$	7.94	C5-A	9

DIMENSIONLESS DOWNSTREAM DISTANCE $\sim \dfrac{x}{b} \dfrac{\Gamma_0}{U_\infty b} (AR)^2 f\left(\dfrac{\Gamma_0}{\nu}\right)$

Fig. 10 Reynolds number function, Eq. (13).

distribution (e.g., elliptic), the maximum velocity V_1 would be proportional to Γ_0 /r_0 or

$$V_1 r_0 /\Gamma_0 \sim V_1 S /\Gamma_0 b = V_1 b /\Gamma_0 AR \cong \text{constant} \qquad (10)$$

in the plateau region. Equation (9) can be rewritten

$$V_1 b /\Gamma_0 AR = C_0 /[(x/b)(\Gamma_0 /U_\infty b)(AR)^2 f(\Gamma_0 /\nu)]^{\frac{1}{2}} \qquad (11)$$

or, including the plateau region

$$V_1 b /\Gamma_0 AR = f_1 [(x/b)(\Gamma_0 /U_\infty b)(AR)^2 f(\Gamma_0 /\nu)] \qquad (12)$$

where

$$f(\Gamma_0 /\nu) = (5.80)^2 /[(V_1 x /\Gamma_0)(\Gamma_0 /U_\infty x)^{\frac{1}{2}}]^2 \qquad (13)$$

Note that the functional relationship Eq. (12) also holds for Eq. (4), if Squire's coefficient a is assumed to be a function of Γ_0 /ν.

Experimental water-channel, wind-tunnel, and flight data from Refs, 1, 6-9, and 16-19 are plotted in terms of

$$V_1 b /\Gamma_0 AR$$

and

$$(x/b)(\Gamma_0 /U_\infty b)(AR)^2 f(\Gamma_0 /\nu)$$

in Fig. 9. The solid line represents a value for

$$V_1 [x /U_\infty \Gamma_0) f(\Gamma_0 /\nu)]^{\frac{1}{2}}$$

of 5.80. The similarity region appears to begin at a value of the abscissa of about 50, corresponding to approximately 12 span-lengths aft of a typical aircraft at a lift coefficient of 1. The function $f(\Gamma_0 /\nu)$ is shown in Fig. 10.

An effective constant eddy viscosity, based on maximum tangential speed and Eq. (4), was calculated from similarity region data and also from the variable eddy viscosity solutions. The results (Fig. 11) show that, for a constant eddy viscosity assumption, Squire's hypothesis [Eq. (1)] is valid for values of $\Gamma_0 /\nu \geq 10^6$. A different value of eddy viscosity would be obtained if circulation Γ_1 or radius r_1 were used as a basis, since the Lamb solution [Eq. (4)], does not well represent velocity profile data or the variable eddy viscosity solution.

A correlation equation, based on Owen's result [Eq. (2)] would result in

$$f(\Gamma_0 /\nu) \sim (\Gamma_0 /\nu)^{-\frac{1}{2}}$$

This equation would approximate Eq. (13) only in a narrow region from $\Gamma_0 /\nu = 10^4$ to $3(10)^4$, and a correlation equation, based on Owen's result, cannot be used to correlate scale-model and flight data.

Conclusion

The numerical solution of the decay of a self-similar line vortex with variable eddy viscosity has been used to derive a correlation function for comparison of scale-model and flight data. It has been shown that for high Reynolds number, the velocity and circulation profiles vary significantly from the constant-eddy-viscosity Lamb solution.

The primary purpose of this investigation is to correlate existing experimental data to ascertain the effect of change in Reynolds number on the characteristics of trailing vortices. Although the eddy viscosity model that is used is not as rigorous physically as more sophisticated closure models, the resulting tangential speed profiles are close to the limited experimental data available. The model thus serves the intended purpose quite well. Plotting the scale-model and flight data in terms of the vortex velocity scaling parameter $V_1 b /\Gamma_0 AR$ vs the distance scaling parameter

$$(x/b)(\Gamma_0 /U_\infty b)(AR)^2 f(\Gamma_0 /\nu)$$

SYM	FACILITY	Γ_0/ν REYNOLDS NO.	AR ASPECT RATIO	MODEL	REFERENCE
○	TOW TANK	$3.9\,(10)^4$	5.33	RECTANGULAR	1
□	TOW TANK	$4.8\,(10)^4$	5.33	RECTANGULAR	1
△	TOW TANK	$7.7\,(10)^4$	5.33	RECTANGULAR	1
◇	WIND TUNNEL	$1.4\,(10)^5$	5.33	RECTANGULAR	17
⌂	WIND TUNNEL	$9.5\,(10)^4$	5.33	RECTANGULAR	17
◣	FLIGHT	$1.3\,(10)^6$	5.62	CHEROKEE	6
◢	FLIGHT	$1.4\,(10)^6$	7.45	O-1	6
◆	FLIGHT	$1.9\,(10)^6$	5.62	CHEROKEE	6
◆	FLIGHT	$3.5\,(10)^6$	6.12	P-51	7
■	FLIGHT	$9.4\,(10)^6 - 1.3\,(10)^7$	6.22	COMET III	8
▲	FLIGHT	$1.9\,(10)^7$	7.94	C5-A	9

FROM NUMERICAL
SOLUTION, eq. (5)

FLIGHT, ref. 6–9

TOW TANK, WIND TUNNEL
ref. 1, 17

RATIO, EFFECTIVE EDDY VISCOSITY TO KINEMATIC VISCOSITY, ϵ/ν
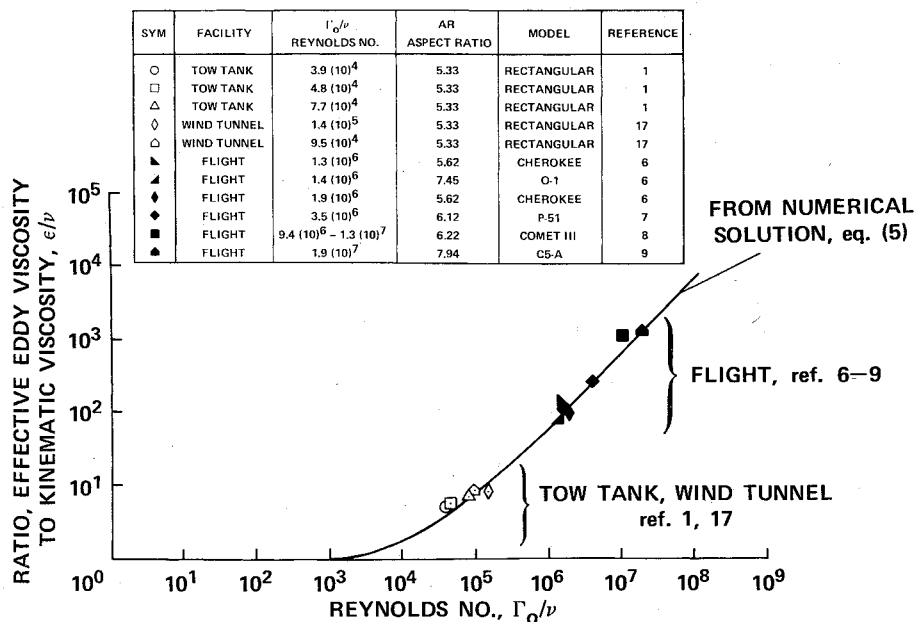
REYNOLDS NO., Γ_0/ν

Fig. 11   Effective viscosity ratio based on constant viscosity solution and core radius velocity.

effectively collapses the data to a single curve. Although there is, of course, much scatter in the data correlated in Fig. 9, the correlation Eq. (12) collapses the data reasonably well, and should serve as a basis for evaluation of future scale-model and flight tests.

References

[1]Ciffone, D. amd Orloff, K., "Far Field Wake Vortex Characteristics of Wings," *Journal of Aircraft*, Vol. 12, May 1975, pp. 464-470.

[2]Squire, H.B., "The Growth of a Vortex in Turbulent Flow," *Aeronautical Quarterly*, Vol. 16, 1965, pp. 302-306.

[3]Lamb, H., *Hydrodynamics,* Dover, New York, 1945, pp. 591-592.

[4]Owen, P.R., "The Decay of a Turbulent Trailing Vortex," *Aeronautical Quarterly*, Vol. 21, 1970, pp. 69-78.

[5]Baldwin, B.S., Chigier, N.A., and Sheaffer, Y.S., "Decay of Far-Flowfield in Trailing Vortices," *AIAA Journal*, Vol. 11, Dec. 1973, pp. 1601-1602.

[6]McCormick, B.W., Tangler, J.L., and Sherrieb, H., "Structure of Trailing Vortices," *Journal of Aircraft*, Vol. 5, May-June 1968, pp. 260-267.

[7]Kraft, C.C., "Flight Measurements of the Velocity Distribution and Persistence of the Trailing Vortices of an Airplane," NACA TN 3377, 1955.

[8]Rose, R. and Dee, F.W., "Aircraft Vortex Effects and Their Effects on Aircraft," Royal Aircraft Establishment TN Aero 2934, 1963.

[9]Dunham, R.C., Verstynen, H.A., and Benner, M.S. (unpublished data), NASA Langley Research Center, 1971.

[10]Hoffman, E.R. and Joubert, P.N., "Turbulent Line Vortices," *Journal of Fluid Mechanics*, Vol. 16, 1963, pp. 395-411.

[11]Govindaraju, S.P. amd Saffman, P.G., "Flow in a Turbulent Trailing Vortex," *Physics of Fluids*, Vol. 14, Oct. 1971. pp. 2074-2080.

[12]Saffman, P.G., "Structure of Turbulent Line Vortices," *Physics of Fluids*, Vol. 16, 1973, pp. 1181-1188.

[13]Donaldson, C. DuP., "Calculation of Turbulent Shear Flows for Atmospheric and Vortex Motions," *AIAA Journal*, Vol. 10, Jan. 1972. pp. 4-12.

[14]Rossow, V.J., "Prediction of Span Loading from Measured Wake-Vortex Structure-an Inverse Betz Method," *Journal of Aircraft*, Vol. 12, July 1975, pp. 626-628.

[15]Spreiter, J.R. and Sacks, A.H., "The Rolling up of the Trailing Vortex Sheet and Its Effect on the Downwash Behind Wings,"-*Journal of the Aeronautical Sciences*, Vol. 18, Jan. 1951, pp. 21-32.

[16]Mather, G.K., "A Note on Some Measurements Made in Vortex Wakes Behind a DC-8," NRC Canada, DME/NAE Quarterly Bulletin, No. 1967 (2) 1967.

[17]Corsiglia, V.R., Schwind, R.G., and Chigier, N.A., "Rapid Scanning, Three-Dimensional Hot-Wire Anemometer Surveys of Wing-Tip Vortices," *Journal of Aircraft*, Vol. 10, Dec. 1973, pp. 752-757.

[18]Marshall, J.R. and Marchman, J.F., "Vortex Age as a Wake Turbulence Scaling Parameter," AIAA Paper 74-36, Washington, D.C., 1974.

[19]Dosanjh, D.S., Gasparek, E.P., and Eskinazi, S., "Decay of a Viscous Trailing Vortex," *Aeronautical Quarterly*, Vol. 13, 1962, pp. 167-188.